Fast AAA Thrombus Segmentation from CTA Images for Endovascular Repair Follow-up

Iván Macía[1,2,3], María Arenas[1,2], Jon Haitz Legarreta[1,2], Isabelle Robin[1,2], Manuel Graña[3], and Sabarinath Rajasekharan[1,2]

[1] Vicomtech Foundation, San Sebastián - Donostia (Spain)
http://www.vicomtech.org
[2] Biodonostia Health Research Center, San Sebastián - Donostia (Spain)
http://www.biodonostia.org
[3] Computational Intelligence Group, University of the Basque Country UPV/EHU
(Spain) http://www.ehu.es/ccwintco

imacia@vicomtech.org

Abstract. Segmentation and quantification of AAAs in CTA images is a relevant task for primary diagnosis and follow-up after EVAR. This paper describes and evaluates a refined version of a fast and accurate method for the segmentation of the aneurysm thrombus based on a radial model approach. It uses a priori knowledge and spatial coherency for obtaining an initial thrombus contour which is then refined by removing spurious sectors. The method provides a fast segmentation and easy parameter setup while maintaining a high degree of accuracy, which makes it suitable for clinical routine. Thrombus segmentation results are presented in real clinical CTA images used for EVAR follow-up which demonstrate the high speed and accuracy of the method.

Keywords: Abdominal aortic aneurysm, AAA, endovascular aneurysm repair, EVAR, Computed Tomography Angiography, CTA, lumen, thrombus, segmentation, radial model

1 Introduction

Abdominal aortic aneurysms (AAAs) are focal enlargements of the aortic wall in the abdominal region of the aorta whose rupture has a high risk of mortality. Endovascular Aneurysm Repair (EVAR) is the preferred surgical procedure, which requires periodic follow-up using CTA images. It has been suggested [1] that the aneurysm volume change is the best indicator to determine positive evolution, which requires a prior segmentation of the thrombus. Segmentation of the aneurysm thrombus is mainly hindered by the presence of adjacent structures with similar intensity on the images and some irregularity in its shape. Thrombus segmentation strategies proposed in the literature include, among others, deformable models [2,3,4], level-set methods [5,6,7] or Active Shape Models (ASM) [8]. Some of these methods give reasonable good results but either they

are too complex to be setup or controlled by a non-expert or depend on the availability of a good set of training data. Moreover, they are time consuming and require some degree of user interaction, sometimes difficult to be implemented within an interface for clinical routine. Dehmeshky *et al.* [9] proposed a grayscale and geometric appearance model [9]. Similarly, we use prior knowledge on the appeareance of the aneurysm, but their method requires masking of several adjacent structures. Recently, segmentations with active contours using polar representations where proposed in [10].

We present some improvements and experimental evidence on our algorithm for AAA thrombus segmentation described in [11]. The proposed method, based on a radial model approach with appearance priors and spatial constraints, is very fast and needs little human interaction for initialization or parameter tuning. An initial thrombus segmentation is obtained starting from the detected lumen or stent boundaries. This segmentation is then corrected using geometrical constraints in order to avoid leakage in adjacent structures where no apparent aneurysm boundary is visible. Its simplicity and speed makes it suitable for clinical routine allowing easy parameter setting with visual feedback, as it is designed as a part of a complete system for EVAR follow-up.

The remainder of this paper is organized as follows. The basic method is described briefly, with some remarks from our recent experience, in Section 2; Section 3 describes some initialization issues. Section 4 describes the general procedure for thrombus contour correction; Section 5 provides experimental results with a discussion in Section 6. Finally, Section 7 presents our conclusions.

2 AAA Segmentation

The complete AAA segmentation method consists of the following stages:

1. *Lumen Segmentation*: an initial lumen segmentation is obtained using a region growing algorithm based on confidence measures from a pair or more seed points as implemented in [12].
2. *Lumen Centerline Extraction*: performed slice by slice using 2D image moments on the connected components (CCs). CCs not corresponding to the lumen are discarded by calculating centroid distances to adjacent slices.
3. *Polar Reformatting*: a slice-based polar reformatting is generated, in order to obtain a linear representation of the radial model which is faster to process. Strictly, this does not constitute a reformatting on cylindrical coordinates but, rather, a generalized cylinder. This allows to adapt to the shape of the centerline, taking into account its curvature. The presence of a dominant vertical direction makes the method still valid.
4. *Initial Thrombus Segmentation*: based on the analysis of connected components (CCs) described both radially and at slice level using run-length encoding. The result is a set of radial contours describing the thrombus outer boundary starting from the inner boundary. It requires a pre-processing step consisting of median filtering, in order to remove noise, and a raw thresholding which removes the hyperintense structure corresponding to the stent

and other spurious structures. Note that, differently from other methods, we do not remove any structure outside the thrombus region. The result is a good approximation of the external thrombus contour, with the exception of some areas where the thrombus region invades adjacent structures.

5. *Thrombus Contour Correction*: based on the analysis of discontinuities in the initial contours and statistical information, outlier sectors in radial contours are identified and replaced by interpolation between valid contour segments.

6. *3D Reconstruction and Smoothing*: introduces some regularization in the axial direction by removing remaining spurious edges.

7. *Volume Quantification*: corresponds to the region from the external part of the stent to the segmented outer thrombus boundary.

We refer the reader to our article on [11] for details on the first four stages. In the next sections, we will focus on the initialization and correction stages which were improved in order to obtain more accuracy and robustness.

3   Initialization Issues

The segmentation of the thrombus may start from a prior lumen segmentation or by automatic detection of the lumen boundaries, as in the experiments performed in this paper. In routine EVAR follow-up CTA images two problems arise during initialization severely affecting the thrombus segmentation: the presence of the stent and the iliac arteries bifurcation.

In our method, we do not deal with the problem of an accurate stent segmentation. However, the segmentation based on CC analysis is less problematic if we first detect the stent and consider the region outside its boundaries. We simply detect the stent as CCs of high intensity in the close vecinity of the lumen. After removal, it is assumed that the thrombus region corresponds to the adjacent area extending radially.

One major problem found during our initial experiments, was the presence of double iliac arteries in the thrombus region as can be seen in Figures 2a and 2c. Most of the methods assume that the thrombus is only present in the aortic area, where there is a single lumen branch. However, the bulge may be present in the area where the iliac arteries start, even when the aneurysm itself was not present in this area before the intervention. In this case, the stent forces the two branches of the iliac arteries to be close to each other and there exist two center-line branches. One solution consists of first segmenting the lumens of both iliac arteries and then extend this segmentation in order to create a convex contour by filling the concave areas between both branches at each slice. This allows us to apply the rest of the segmentation algorithm for the thrombus without further modification. The convex contour may be obtained easily using open and close morphological operations. In practice, complete convexity is not always needed for the algorithm to work (see Figure 2c where the mask is overlaid).

4   Thrombus Contour Correction

Thrombus contour correction has been improved from the implementation in [11], by introducing a bias correction in the thrombus center position, which improves results when the lumen is not centered with respect to the thrombus, and two parameters that control the correction of spurious radial sectors.

The external thrombus contour correction is based on a continuity constraint imposed over the external contour T_{ext}. We assume that the thrombus is radially smooth, allowing for small discontinuities which are first identified as significant radial changes from point to point by using a discontinuity parameter δ.

In the initial radial function, there exist some bias due to the offset of the centerline with respect to the geometric center of the thrombus, which is unknown. In order to partially remove this bias, we first recompute the centroid of the initial contour and update the angles, which yields a new radial function T'_{rext} for the external contour in which discontinuities are easier to identify.

After the identification of discontinuities, the contour is divided in radial sectors $S_i(\theta_i, \theta_{i+1})$ defined as

$$S_i(\theta_i, \theta_{i+1}) = \{T'_{rext}(\theta) : \theta \in [\theta_i, \theta_{i+1}]\} :$$
$$|T'_{rext}(\theta_i) - T'_{rext}(\theta_{i-1})| > \delta, \quad |T'_{rext}(\theta_{i+1}) - T'_{rext}(\theta_i)| > \delta \tag{1}$$

Next we identify the spurious radial sectors. We calculate their average values comparing them with the standard deviation from the median of all radial values. That is, we mark a sector S_i as spurious if:

$$\mu(S_i) > \kappa \sigma_{median}(T'_{rext}) \tag{2}$$

where κ is a scaling factor and $\sigma_{median}(T'_{rext})$ is the standard deviation of the median of radius values. Using the median instead of the mean, prevents outlier values from influencing the calculations. Confirmed contiguous radial sectors are joined to obtain new sectors. Finally, discarded radial sector values are replaced by linearly interpolating the radius between the boundary values of adjacent valid sectors. The procedure is depicted in Figure 1. Note how the correction removes the spurious sectors and how some small discontinuities are preserved, that appear naturally in the thrombus due to the presence of adjacent structures. If necessary, this can be adjusted with the discontinuity parameter δ.

5   Experiments and Results

Our method has been initially tested on 5 CTA datasets from real patients under follow-up after EVAR, obtained from a LightSpeed16 CT scanner (GE Medical Systems, Fairfield, CT, USA) with an average 0.725x0.725x0.8 mm. spatial resolution. Average computation times for thrombus segmentations obtained on an Intel Core 2 Quad CPU at 2.4 Ghz are shown in Table 1. We obtained an average computation time of 0.045 s. per slice demonstrating the high speed of the method. From this total time, on average, 15% was spent calculating the polar reformatting, 47% in the median filtering and 38% in the contour estimation.
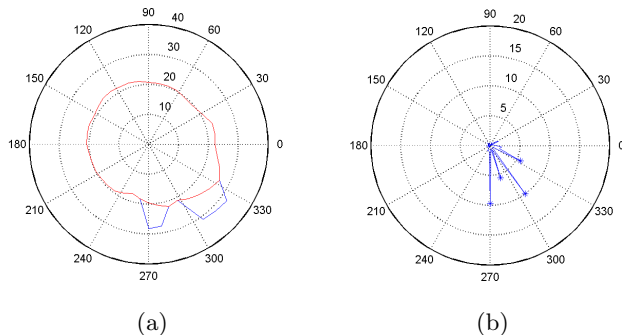
Fig. 1: Contour correction procedure. (a) Initial (blue) and corrected (red) contours of two slices in a polar plot. (b) Corresponding derivative of initial contour and identified discontinuities.

Manual segmentations were carefully delineated by a single expert for comparison. A volume of interest was defined to reduce memory requirements and two seed points inside the lumen were selected for the segmentation of the lumen. The polar representation of the image was obtained in an area of 10 mm around the centerline. The described radial approach was used to segment the thrombus contours and finally a mask was obtained by rasterization of the contour. In all our experiments, we used 40 angular and 250 radial samples respectively (0.4 mm. radial resolution) for the polar reformatting.

The parameters for the initial thrombus segmentation *were not changed* in our experiments. For the correction step we used values of δ in the range 1.5-3.5. The scaling factor κ was fixed to 1.5 except in one dataset which was 2.5. This allowed us to verify that the parameter sensitivity is low, which is good for routine applications. The results were accurate except in some slices with spurious structures that showed no visible boundaries with respect to the thrombus.

Average overlapping ratios of automated A and manual B segmentations are shown in Table 2. The first dataset is a typical case of a thrombus segmentation that our method solves with high accuracy (overlapping ratios of 93.52% and 86.76%). The four other datasets are from the follow-up of a single patient and can be considered a difficult scenario. The thrombus has a region with double lumen in the iliac arteries and the lumen is very eccentrical. Yet good values are obtained. We also present some filtered values where we removed the slices were the contour was leaking in a few contour points in order to test the accuracy in the remaining slices. This can be done either by changing the parameter values for those slices or by manual correction of the contour. Finally, we present a 3D reconstruction of the contours, depicted in Figure 3. We do not provide comparison of volumetric quantifications, since the external stent contour was not available on the manual segmentations. In any case, the focus of this paper is on the external contour, which is the most complicated task.

Dataset	Slices	Time(s.)
1	19	0.87±0.02
2	19	0.87±0.02
3	22	1.02±0.02
4	21	1.01±0.04
5	207	7.68±0.08

Table 1: Computation times for thrombus segmentations in 5 datasets calculated as averages of 10 executions.

Dataset	(a)	(b)	(c)	(d)
1	93.5±2.5	86.8±5.2	-	-
2	89.9±7.3	83.6±7.1	95.4±2.7	89.8±3.4
3	94.0±8.9	83.9±10.5	96.1±2.3	89.1±3.5
4	89.9±9.3	81.9±10.3	95.0±2.4	88.8±3.0
5	92.1±6.7	79.7±9.6	94.0±5.7	86.7±4.3

Table 2: Overlapping areas in % between proposed method segmentations and ground-truth manual segmentations. (a) = B/A$\bigcup$B, (b) = A$\bigcap$B/A$\bigcup$B. (c)=(a) and (d)=(b) both after removing incorrect contours. Table shows average values for all slices in each datasets.

6   Discussion

One of the main advantages of the described method is its efficiency, as it can process a large number of slices in a few seconds with high accuracy (Figure 2). The parameter setting is minimal and most of our experiments have used the same set of parameters. The value of δ could be changed in order to allow for some tolerance in discontinuities. Increasing the value of κ allows more deviation from the median radius value, in cases where the thrombus is very eccentrical with respect to the centerline.

The method provides accurate results where other methods would fail due to absence of visible thrombus boundaries (Figure 2). It also allows for some discontinuities that improve the accuracy with respect to some methods based on smooth curves or deformable models which involve complex calculations.

We emphasize that the method is oriented for the segmentation of AAAs by non image processing experts. The use of a radial approach, makes it very easy to develop a user interface for fast segmentation of CTAs. Parameter setting is relatively simple and the speed of the method allows for quick visual feedback. In case of failure, δ and κ could be adjusted for single slices (however, note that, in our experiments, we used fixed values of δ and κ for all slices of each dataset). If the problems persist, the user simply would have to invalidate possible incorrect regions of the contour and mark only a few radial points at each erroneous section, either manually or by providing the radius value. This has been a major

consideration in the design of the method, since we expect it to be part of a software for follow-up of EVAR interventions.

The method works on a slice-by-slice basis in order to take into account the symmetry with respect to the centerline and to reduce the possibility of large leaks at volumetric level, where some coherence is introduced by the 3D polygonal smoothing. The polar representation is also advantageous, since it presents the data in the form of a generalized cylinder VOI around the centerline, which implicitly takes into account the radial symmetry, and allows fast calculations based on CCs and run-length encoding.

7   Conclusions

We have developed a method for fast segmentation of AAAs after EVAR interventions. First, the lumen of the aorta is segmented and a centerline is obtained. The thrombus segmentation uses a radial model and is obtained by analysis of connected components subject to spatial constraints and prior knowledge. The thrombus correction stage is based on dividing the initial external contours obtained from the thrombus in radial sectors according to discontinuities found along the contour. Then the incorrect sectors are discarded according to statistical measurements and the gaps interpolated according to adjacent sectors. We show initial experimental evidentce on five real CTA datasets. We also consider the case where the iliac artery bifurcation is inside the thrombus region. The method is very fast while maintaining a high degree of accuracy, requires minimal parameter setting, since most of the possible parameters remain fixed and thus is suitable for clinical routine. Future work will be oriented to further improve the robustness of the method, regularize resulting contours on a final stage and perform a more exhaustive clinical validation.

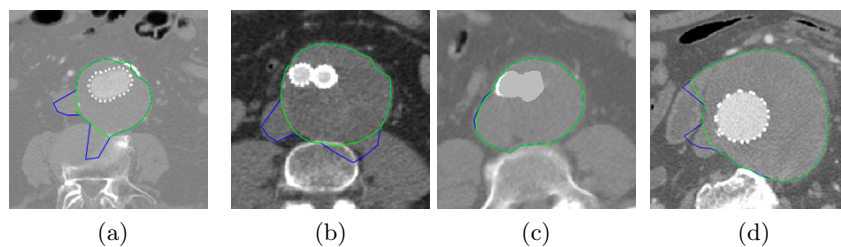(a)   (b)   (c)   (d)

Fig. 2: Segmented slices by our approach showing the initial (blue) and the corrected (green) contours. Figure (d) shows some problems found.
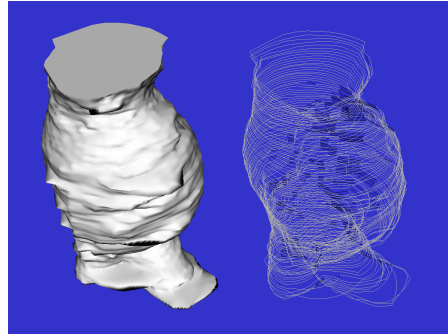
Fig. 3: 3D polygonal reconstruction (left) and 3D contours (right) for dataset 1.

References

1. Wever, J., Blankensteijn, J., Mali, W., Eikelboom, B.: Maximal aneurysm diameter follow-up is inadequate after endovascular abdominal aortic aneurysm repair. European J. of Vasc. and Endovasc. Surg. **20** (2 2000) 177–182
2. Subasic, M., Loncaric, S., Sorantin, E.: 3d image analysis of abdominal aortic aneurysm. In: Proc. SPIE Med. Imag. Proc. Volume 4684. (2002) 1681–9
3. Olabarriaga, S., Rouet, J., Fradkin, M., Breeuwer, M., Niessen, W.: Segmentation of thrombus in abdominal aortic aneurysms from cta with nonparametric statistical grey level appearance modelling. IEEE Trans. Med. Imag. **24** (4 2005) 477– 485
4. Demirci, S., Lejeune, G., Navab, N.: Hybrid deformable model for aneurysm segmentation. In: IEEE Int. Symp. on Biomedical Imaging: From Nano to Macro, Boston, Massachusetts, USA (June/July 2009)
5. Zohios, C., Kossioris, G., Papaharilaoub, Y.: Geometrical methods for level set based abdominal aortic aneurysm thrombus and outer wall 2d image segmentation. Computer Methods and Programs in Biomedicine **107**(2) (2012) 202–217
6. Zhuge, F., Rubin, G., Sun, S., Napel, S.: An abdominal aortic aneurysm segmentation method: level set with region and statistical information. Med. Phys. **33** (5 2006) 1440–53
7. Das, B., Mallya, Y., Srikanth, S., Malladi, R.: Aortic thrombus segmentation using narrow band active contour model. In: Proc. IEEE Eng. Med. Biol. Soc. Volume 1. (2006) 408–11
8. de Bruijne, M., van Ginneken, B., Viergever, M., Niessen, W.: Interactive segmentation of abdominal aortic aneurysms in cta images. Med.Im.An **8** (2004) 127–38
9. Dehmeshki, J., Amin, H., Ebadian-Dehkordi, M., Jouannic, A., Qanadli, S.: Automatic detection, segmentation and quantification of abdominal aortic aneurysm using computed tomography angiography. In: Proc. Med. Image Understanding and Analysis. (2009)
10. Baust, M., Yezzi, A., Unal, G., Navab, N.: A sobolev-type metric for polar active contours. In: Proc. Comp. Vis. Pattern Recognition (CVPR). (2011) 1017–24
11. Macía, I., Graña, M., Maiora, J., Paloc, C., de Blas, M.: Detection of type ii endoleaks in abdominal aortic aneurysms after endovascular repair. Computers in Medicine and Biology **41**(10) (Oct 2011) 871–89
12. Ibanez, L., Schroeder, W., Ng, L., Cates, J.: The ITK Software Guide 2nd Ed. Kitware, Inc. ISBN 1-930934-15-7. (2005)